Nigerian Journal of Science and Environment 2025 Volume 23 (1) 134 – 144 ISSN: 3043 – 4440
https://doi.org/10.61448/njse2312511

Influence of deposition temperature on the bandgap energy and optical characteristics of electrochemically prepared SrSe/ZrSe heterostructure

Agbrara, A.I.[a], Emuvokeraye, O.S.[b], Osiele, M.O.[a] and Ikhioya, I.L[c,*]
[a] Department of Physics, Delta State University, Abraka. Delta State, Nigeria.
[b] Department Physics, Dennis Osadebay University Asaba, Delta State, Nigeria.
[c] Department of Physics, Federal University Lokoja, Kogi State, Nigeria
*Corresponding author: ikhioyalucky@gmail.com

Abstract

The thermoelectric advantages of chalcogenides allow for the conversion of temperature fluctuations into electrical voltage. On the other hand, thermoelectgric generators and coolers make use of strontium selenide (SrSe) and zirconium selenide (ZrSe) to enhance their energy efficiency and heat recovery in industries. In this study, the electrochemical deposition technique was employed to synthesize the SrSe/ZrSe heterostructure and to show its potential applications in electronic industries. The XRD spectrum reveals a polycrystalline cubic structure with diffraction angles of 11.93°, 13.87°, 20.71°, and 27.87° at 2 thetas. Introducing ZrSe into SrSe to form the heterostructural films enhanced the crystallinity of films, as seen from the increased peak intensity. The lowest absorbance of 2.22 eV was obtained at 50 °C for the SrSe/ZrSe heterostructure prepared using electrochemical deposition, while the pure film had a slightly higher absorbance of 2.50 eV. The absorbance of the films increases with higher precursor temperatures, showing the strong impact of temperature on synthesis. A decrease in bandgap energy from 2.37 eV to 2.22 eV resulted from SrSe/ZrSe synthesis across precursor temperatures of 40°C to 50°C, respectively.

Keywords: SrSe/ZrSe heterostructure band gap; precursor temperature; absorbance.

Introduction

The combination of transition metals with chalcogen elements like sulfur, selenium, and tellurium gives rise to transition metal chalcogenides (TMCs). The outstanding features of these materials in electronics, optics, and structure have aroused a great deal of interest in recent times *(*Jiang *et al*., 2002; Joo *et al*., 2001; Kundale *et al*., 2023; Lee *et al*., 1969; Mousavi *et al.*, 2023; Muhammad *et al*., 2020). Their ability to excel in multiple areas is showcased in electronics, optoelectronics, catalysis, and energy storage. Transition metal chalcogenides usually have layered structures where its atoms are sandwiched between chalcogen layers. This layered architecture makes it easier to exfoliate into 2D materials, such as graphene. MoS_2, WSe_2, and TiS are among the commonly found TMCs (Bhattacharyya, 2015; Ding *et al*., 2016; Golub *et al*., 2003). The potential to regulate these layers at an atomic level brings about new material properties and functionalities. TMCs can display a broad range of electronic properties, from semiconducting to metallic behavior, depending on their composition and structure. Hence, diverse applications in modern technology rely on chalcogenide materials. Their individual qualities and capacity for innovation make them a primary subject of study in materials science research, resulting in a constant growth of applications across diverse industries. The technology requires that Electropositive elements are combined with a chalcogen element (S, Se, or Te) to form chalcogenide with diverse chemical compositions and unique physical and electrical/electronic properties. Hence, they can be used in various applications in electronics, optics, and numerous energy fields. Chalcogenide compounds can be binary, ternary, or quaternary. The most fundamental instances of binary chalcogenides include CdS, SrSe, ZrSe, and PbSe (Nag *et al*., 2023). Compounds like copper indium gallium selenide (CIGS) are commonly utilized in the complex structures of solar cells. The variability in crystal structures can influence the electronic and optical properties of these materials. The presence of chalcogenides allows for the formation of heterojunctions and the manifestation of optoelectronic properties like photoconductivity and photoluminescence. Their attributes make them well-suited for photodetectors, light-emitting devices, and solar cells. The advancement of thin-film photovoltaic technology owes a lot to CdTe and CIGS materials (Peter Papoh, 2019). Chalcogenides also display advantageous thermoelectric features, enabling them to convert temperature variations into electric voltage and vice versa. The widespread application of strontium selenide (SrSe) and zirconium selenide (ZrSe) in thermoelectric generators and coolers across industries leads to improved energy efficiency and waste heat recovery.

A new technique for producing strontium selenide through selenium reduction was demonstrated by Arellano *et a*l (Arellano-Tánori *et al.*, 2014). The oxidation of selenium from stage 0 to -2 is followed by its combination with strontium chloride, a salt of strontium. This technique achieves a swift exchange of chemical reactions. By measuring adsorption in the UV-visible range, the optical characterization allowed for the computation of direct and indirect band gap energies. Suspended in a water-based solution, the resulting strontium selenide is a black powder with Band gap values of 5.19 and 4.53 eV for direct and indirect, respectively. By analyzing the Raman spectrum, it was determined that there are three peaks: 114 cm^{-1} and 234 cm^{-1}, suggesting the presence of strontium selenide, and 456 cm-1, suggesting the presence of strontium oxide. The existence of strontium oxide, along with O-H and H-O-H vibrations, is indicated by the infrared response observed at 615 cm^{-1}. Finally, transmission electron microscopy has exposed the existence of a crystalline structure. In their study, Kumar *et al* (Kumar *et al*., 2015) revealed that SrSe can be synthesized at temperatures as low as 220 °C without altering its microscale morphology and luminescent properties. The room temperature luminescent data indicates that the decrease in anionic vacancies is accountable for the blue and red emissions observed when doped with Eu2+ and Eu^{3+} respectively. SEM analysis indicates that fabricated SrSe has microrods (Eu^{3+}) and micro spindles (Eu^{2+}) morphology, characterized by micro-scale dimensions. The ability to synthesize doped SrSe microcrystals at low temperatures in a scalable manner can pique interest in their usage in optical sensor devices and solid-state lighting technology.

In this study, the electrochemical deposition technique was employed to synthesize the SrSe/ZrSe heterostructure, demonstrating its potential applications in the electronic industries. To evaluate their photovoltaic potential, the films underwent characterization using UV-visible spectroscopy, X-ray diffraction, and four-point probe.

Material and Methods

Materials used

A number of chemicals were used for the synthesis and characterization of SrSe/ZrSe heterostructure. These include Zirconium (IV) oxychloride octahydrate ($ZrOCl_2.8H_2O$), strontium chloride ($SrCl_2.6H_2O$), selenium (IV) oxide (SeO_2), hydrochloric acid (HCl), distilled water, fluorine doped tin oxide (FTO), (0.1 mol, 15 ml) of strontium chloride ($SrCl_2.6H_2O$), (0.1 mol, 15 ml) of Zirconium (IV) oxychloride octahydrate ($ZrOCl_2.8H_2O$) and (0.1 mol, 15 ml) of selenium (IV) oxide (SeO_2).

Synthesis of SrSe/ZrSe heterostructure.

The electrochemical deposition chamber in Figure 1 involved the use of a DC power supply to connect a three-electrode cell. The cell was comprised of a platinum counter electrode, Ag/AgCl reference electrode, and FTO working electrode. Throughout the deposition process, the precursor temperature was varied between 40, 45, and 50^oC, with a steady duration of 10 seconds. The investigations were performed at an unchanging temperature in the room. A potentiostat window was employed to test the SrSe/ZrSe heterostructure films at 29 °C and 4.8 pH for 5 seconds. The applied potential was measured as -210 mV with respect to a saturated calomel electrode. The deposition process involved placing solvents in a 100-ml beaker at 10 V, followed by heating the resulting samples at 210 ^oC for 40 mins to alleviate material tension. X-ray diffractometry was used to analyze the crystal structures and orientations of the films.

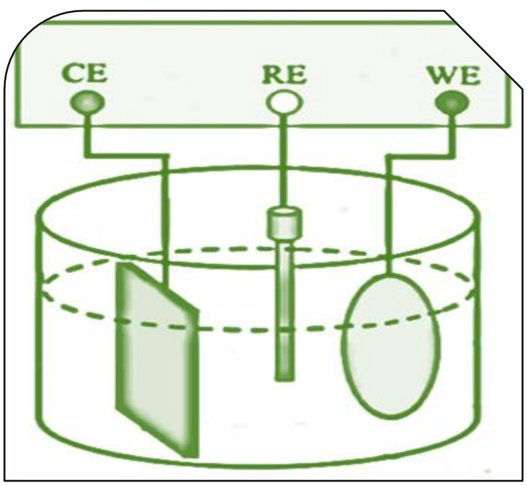

Figure 1: Schematic diagram of the electrochemical deposition chamber used.

Characterization of the materials

The optical, structural, and surface morphology of the deposited films were extensively studied using appropriate equipment and techniques. Using a 756S UV-Visible spectrophotometer, measurements of the absorbance wavelength were taken from 300 nm to 110 nm in the optical spectral ranges. SEM technique was employed to analyze the surface morphology and chemical composition of the films. The Jandel four-point probe technique was employed to analyze the electrical properties of SrSe/ZrSe films. The electrical

characteristics were determined through the measurement of voltage changes across the inner probes and the passing of current between the outer probes. The thin films grown at room temperature were analyzed for sheet resistivity and conductivity.

Result and discussions

Optical analysis of SrSe/ZrSe

Figure 2 [a] demonstrate the correlation between absorbance and wavelength during film deposition at different precursor temperatures. As the film's wavelength increases, its absorbance decreases in both electromagnetic radiation regions. The lowest absorbance was found at 40 ^oC for the material deposition, while the pure film had a slightly higher absorbance. The films' absorbance increases with higher precursor temperatures, showing the strong impact of temperature on synthesis. Typically, films can be used for photovoltaic applications. The absorbance of SrSe/ZrSe heterostructures is influenced by the precursor temperature, which affects various parameters such as crystallization quality, band gap energy, morphology, phase composition, defects, and optical transitions. To achieve desired optical properties in applications like photovoltaics or photodetectors, it is essential to optimize this temperature. Figure 2 [b] illustrate the relationship between transmittance and wavelength during film deposition at different precursor temperatures. In both electromagnetic radiation domains, the film's transmittance increases as its wavelength becomes longer. The highest transmission was observed in the material deposited at 50 ^oC, with the pure film showing a slightly higher transmittance. The rise in precursor temperature leads to an increase in the films' transmittance, demonstrating the significant role of temperature in the synthesis process. Generally, films are a good fit for photovoltaic applications. In Figure 2 [c], the reflectance curve demonstrates the impact of precursor temperature on film deposition as a function of wavelength. As the film's wavelength increases, the reflectance shows an increase in both electromagnetic radiation zones. The reflectivity of the pure film was found to be somewhat higher, in contrast to the material deposited at 50 ^oC, which had the lowest reflectance. The study demonstrates the significant influence of temperature on synthesized films, proving that higher precursor temperatures lead to increased film reflectance. Films are typically suitable for use in photovoltaic applications. The increase in precursor temperature causes changes in optical properties, including absorption and reflectance, due to increased atom mobility. The impact on applications in photonic devices is directly related to the resulting characteristics of the thin film. The performance of SrSe/ZrSe heterostructures can be optimized by carefully controlling the precursor temperature, because there is a correlation between thermal conditions during synthesis and the materials' optical responses.

Nigerian Journal of Science and Environment 2025 Volume 23 (1) 134 – 144 ISSN: 3043 – 4440
https://doi.org/10.61448/njse2312511

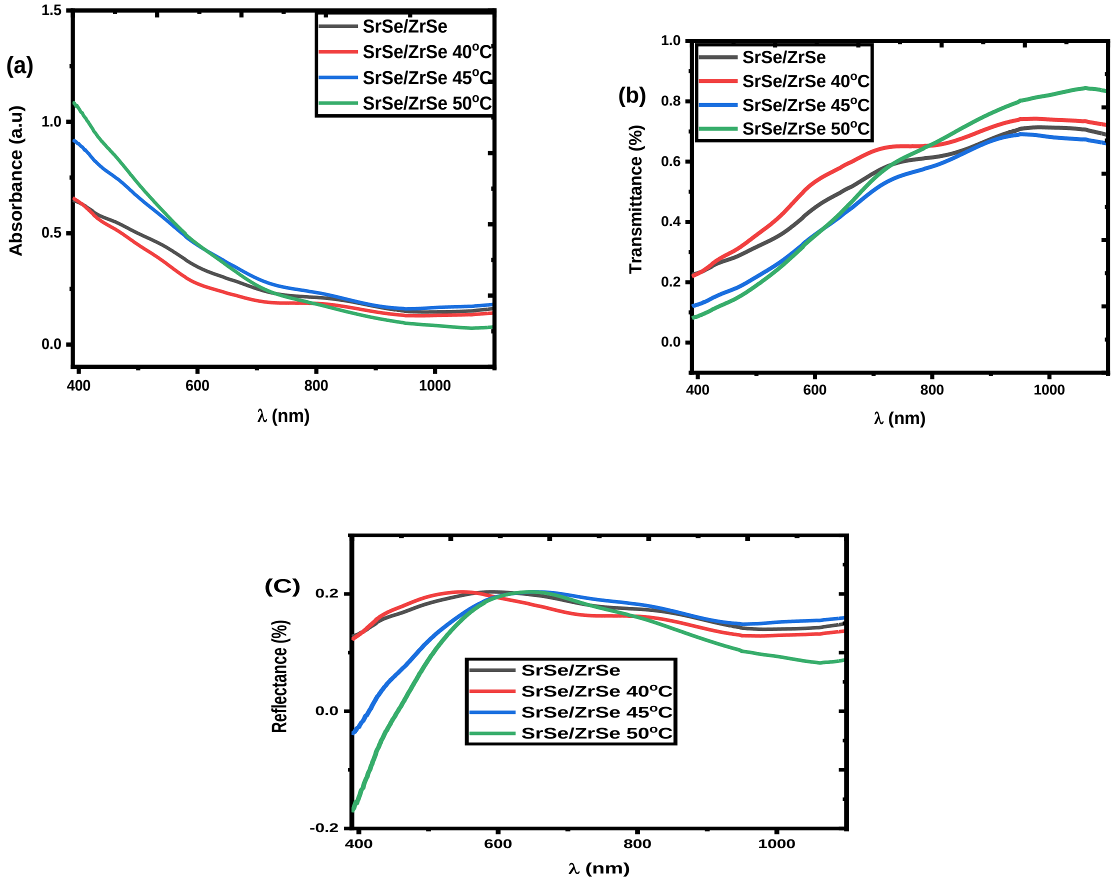

Figure 2: Plot of [a]-absorbance Vs wavelength, [b]-transmittance Vs wavelength, and [c]-reflectance Vs wavelength

Figure 3 illustrates how the absorption coefficient square varies with photon energy for films made at different precursor temperatures. The synthesized SrSe/ZrSe material has a bandgap energy of 2.50 eV. Synthesizing SrSe/ZrSe at different precursor temperatures decreased the bandgap energy from 2.37 to 2.22 eV. A graph depicting the extrapolation of absorption coefficient squared and photon energy.

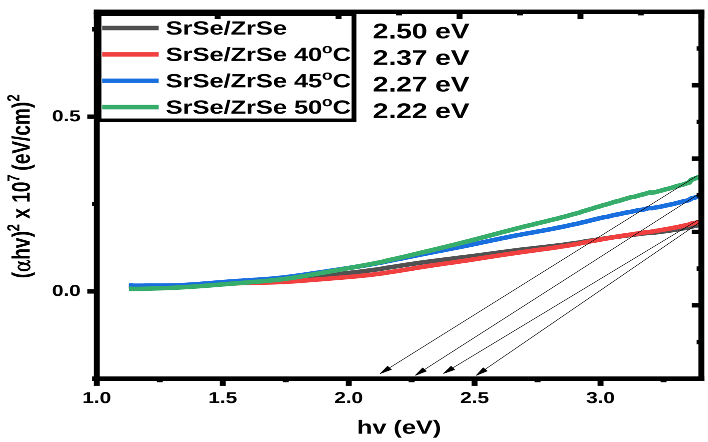

Figure 3: Plot of absorption coefficient square Vs photon energy

The refractive index curve for film deposition at different precursor temperatures is shown in Figure 4 [a]. The film's higher photon energy leads to an increase in the refractive index of the material in both spectral regions. The material placed at 50°C had the lowest refractive index, while the pure film had a slightly higher refractive index (Agbrara *et al*., 2023; Ikhioya *et al*., 2015). The correlation between rising precursor temperatures and increased film reflectance underscores the impact of temperature on synthetic films. Figure 4 [b] display the extinction coefficient as a function of photon energy at different film deposition precursor temperature. The extinction coefficient of the film increases in both spectral regions as photon energy rises. The material deposited at 50°C had the highest extinction coefficient, while the pure film had a slightly higher extinction coefficient. Increasing the precursor temperature leads to higher extinction coefficients in the films, highlighting the significant influence of temperature on synthesize films.

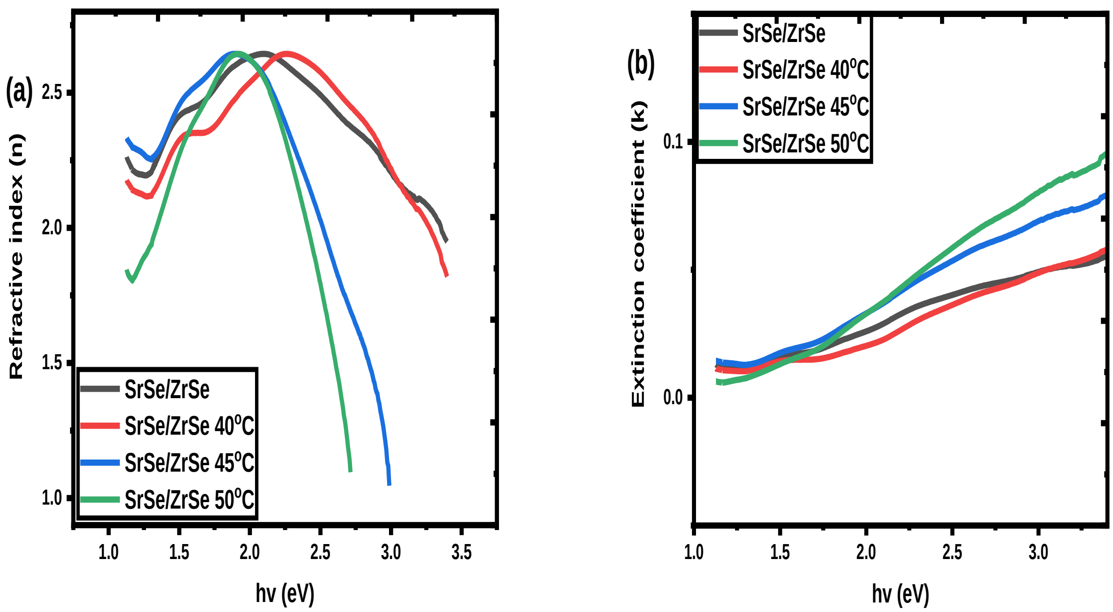

Figure 4: Plot of [a]-refractive index and [b]-extinction coefficient Vs photon energy

Electrical properties of SrSe/ZrSe

Table 1 summarizes the film thickness and electrical properties of SrSe/ZrSe heterostructure at various precursor temperatures, showing a strong correlation between voltage and electrical parameters as well as thickness. As the deposition voltage increases from 40°C to 50°C, the films' thickness increases from 208.98 nm to 211.76 nm, resulting in a higher electrical resistivity and lower electrical conductivity. Figure 5 depicts the correlation between film thickness and the relationship between resistivity and conductivity (Ijeh *et al.*, 2020; Ikhioya *et al.*, 2015, 2020, 2023; Ikhioya *et al.*, 2020). SrSe/ZrSe thin materials are ideal for solar cells and photovoltaic applications due to their high conductivity.

Table 1: Electrical features of SrSe/ZrSe

Materials	Thickness, t (nm)	**ρ** (Ω.m)x 10^4	**σ** (S/m)x 10^3
SrSe/ZrSe	208.98	32.67	30.60
SrSe/ZrSe 40°C	209.42	32.98	30.32
SrSe/ZrSe 45°C	210.86	33.87	29.52
SrSe/ZrSe 50°C	211.76	34.43	29.04

Nigerian Journal of Science and Environment 2025 Volume 23 (1) 134 – 144 ISSN: 3043 – 4440
https://doi.org/10.61448/njse2312511

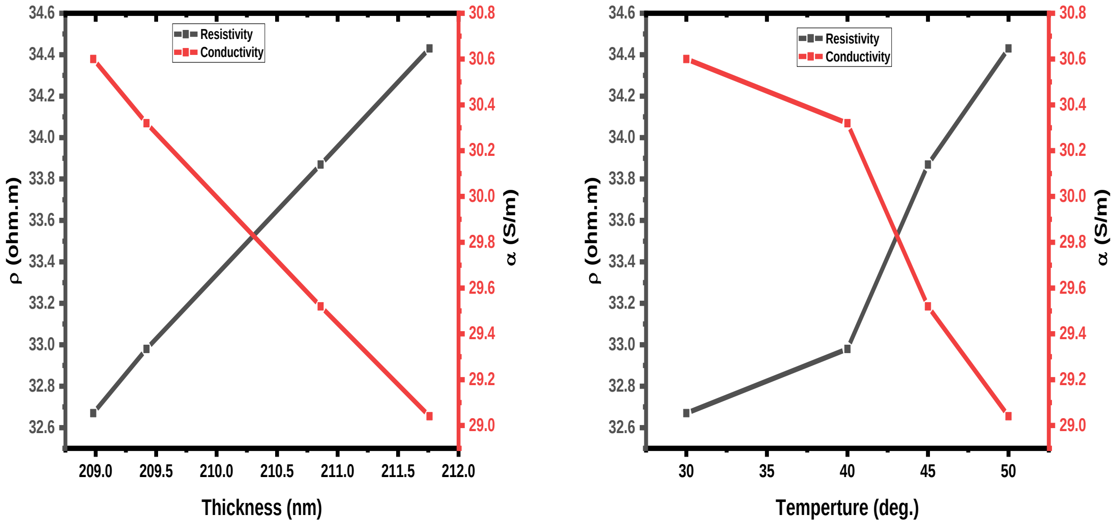

Figure 5: Plot of resistivity and conductivity against thickness & Temperature

The phase analysis of SrSe/ZrSe heterostructure materials

The XRD spectrum of SrSe/ZrSe heterostructure materials deposited at different precursor temperatures of 40^{o}C, 45^{o}C, and 50^{o}C are displayed in Figure 6 with the presence of (101), (102), (111), and (112) crystal planes. The XRD spectrum reveals a polycrystalline cubic structure with a diffraction angle at 2 thetas 11.93^{o}, 13.87^{o}, 20.71^{o}, and 27.87^{o}.The introduction of ZrSe to form the heterostructure films was observed to improve the crystallinity of films as seen from the increased peak intensity. Ikhioya *et al.*, (2015) also reported cubic structures after synthesizing ZnS/CdS heterostructure films via the electrochemical deposition technique. The data gotten during XRD analysis was used in the evaluation of some structural parameters as shown in Table 2

Nigerian Journal of Science and Environment 2025 Volume 23 (1) 134 – 144 ISSN: 3043 – 4440
https://doi.org/10.61448/njse2312511

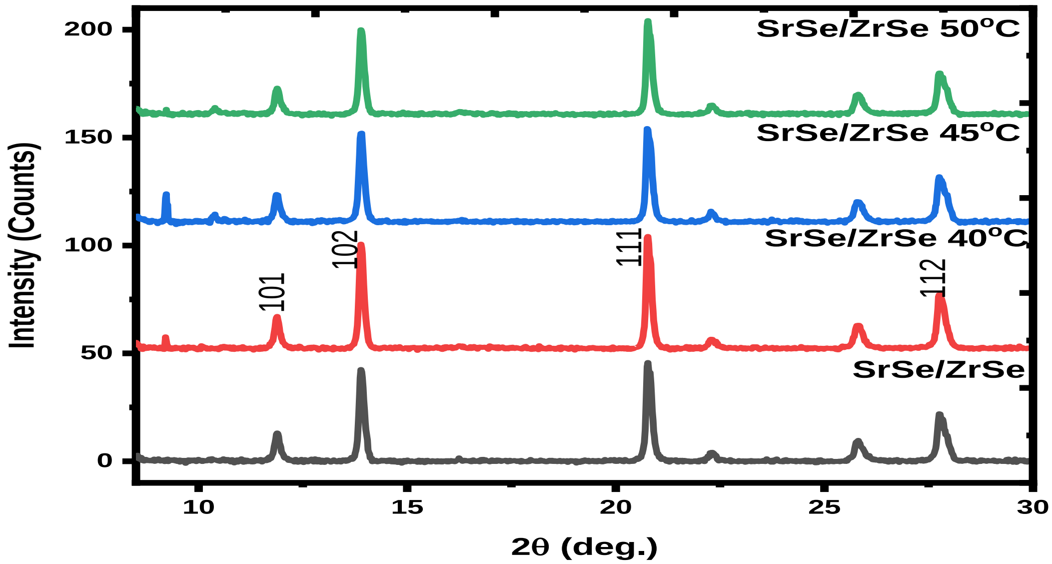

Figure 6: XRD pattern of SrSe/ZrSe

Table 2: Structural parameters

Materials	2θ (deg.)	hkl	d-spacing (Å)	a	β	D (nm)	**σ**
SrSe/ZrSe	11.93	101	7.411	12.836	0.432	3.227	2.925
SrSe/ZrSe 40°C	13.87	102	6.401	12.803	0.465	3.003	3.376
SrSe/ZrSe 45°C	20.71	111	4.284	8.569	0.467	3.018	3.343
SrSe/ZrSe 50°C	27.87	112	3.198	7.151	0.468	3.052	3.269

Conclusion

The electrochemical deposition technique was successfully used to synthesize SrSe/ZrSe heterostructure materials for photovoltaic applications. In both electromagnetic radiation domains, the transmittance of the films increases as the increase in its wavelength. The highest transmission was observed in the material deposited at 50 °C, with the pure film showing a slightly higher transmittance. The rise in precursor temperature leads to an increase in the films' transmittance, demonstrating the significant role of temperature in the synthesis process. The increase in precursor temperature causes changes in optical properties, including absorption and reflectance, due to increased atom mobility. The impact on applications in photonic devices is directly related to the resulting characteristics of the thin film. The performance of SrSe/ZrSe heterostructures can be optimized by carefully controlling the precursor temperature, as studies have shown a correlation between thermal conditions during synthesis and the materials' optical responses. The XRD spectrum of SrSe/ZrSe heterostructure materials deposited at different precursor temperatures of 40^{o}C, 45^{o}C, and 50^{o}C reveals (101), (102), (111), and (112) crystal planes.

References

Agbrara, A. I., Ojegu, E. O., Osiele, M. O., & Ikhioya, I. L. (2023). Electrochemically Synthesize SrSe/ZrSe Heterostructure Material for Photovoltaic Application. *Advanced Journal of Chemistry, Section A*, *6*(4), 401–411. https://doi.org/10.48309/AJCA.2023.407032.1385

Arellano-Tánori, O., Rojas-Hernández, A., Gómez-Fuentes, R., Ochoa-Landin, R., Berman-Mendoza, D., Mendivil-Reynoso, T., Ramírez-Rodríguez, L. P., & Castillo, S. J. (2014). Novel synthesis of SrSe by reduction of selenium into rongalite solutions. *Journal of Ovonic Research*, *10*(2), 55–59.

Bhattacharyya, B. (2015). Electrochemical Machining. *Electrochemical Micromachining for Nanofabrication, MEMS and Nanotechnology*, 25–52. https://doi.org/10.1016/b978-0-323-32737-4.00002-5

Ding, G., Gao, G. Y., Huang, Z., Zhang, W., & Yao, K. (2016). Thermoelectric properties of monolayer MSe2 (M = Zr, Hf): Low lattice thermal conductivity and a promising figure of merit. *Nanotechnology*, *27*(37). https://doi.org/10.1088/0957-4484/27/37/375703

Golub, A. S., Zubavichus, Y. V., Slovokhotov, Y. L., & Novikov, Y. N. (2003). Monolayer dispersions of transition metal dichalcogenides in the synthesis of intercalation compounds. *Uspekhi Khimii*, *72*(2), 138–158. https://doi.org/10.1070/rc2003v072n02abeh000789

Ijeh, R. O., Nwanya, A. C., Nkele, A. C., Madiba, I. G., Bashir, A. K. H., Ekwealor, A. B. C., Osuji, R. U., Maaza, M., & Ezema, F. (2020). Optical, electrical and magnetic properties of copper doped electrodeposited MoO3 thin films. *Ceramics International*, *46*(8), 10820–10828. https://doi.org/10.1016/j.ceramint.2020.01.093

Ikhioya, I. L., Aisida, S. O., Ahmad, I., & Ezema, F. I. (2023). The effect of molybdenum dopant on rare earth metal chalcogenide material. *Chemical Physics Impact*, *7*(April), 100269. https://doi.org/10.1016/j.chphi.2023.100269

Ikhioya, I. L., Nkele, A. C., Okoro, C. F., Obasi, C., Whyte, G. M., Maaza, M., & Ezema, F. I. (2020). Effect of temperature on the morphological, structural and optical properties of electrodeposited Yb-doped ZrSe2 thin films. *Optik*, *220*. https://doi.org/10.1016/j.ijleo.2020.165180

Ikhioya, I. L., Okanigbuan, P. N., Agbakwuru, C. B., & Osolobri, B. U. (2015). Journal of the Nigerian Association of Mathematical Physics © J . of NAMP Characterization of Zinc Sulphide / Cadmium Sulphide (ZnS / CdS) Superlattice by Electrodeposition Technique of Physics and Industrial Physics , Nnamdi Azikiwe University , Awka ,. *Journal of the Nigerian Association of Mathematical Physics*, *29*, 331–338.

Ikhioya, L. I., Chime, U. K., Okoro, C. F., Iroegbu, C., Maaza, M., & Ezema, F. I. (2020). Influence of dopant concentration on the electronic band gap energy of Yb-ZrSe2 thin films for photovoltaic application via electrochemical deposition technique. *Materials Research Express*, *7*(2). https://doi.org/10.1088/2053-1591/ab7690

Jiang, L. F., Shen, W. Z., & Wu, H. Z. (2002). Optical properties of SrSe thin films grown by molecular beam epitaxy. *Journal of Applied Physics*, *91*(11), 9015–9018. https://doi.org/10.1063/1.1474593

Joo, J., Lee, J. K., Baeck, J. S., Kim, K. H., Oh, E. J., & Epstein, J. (2001). Electrical, magnetic, and structural properties of chemically and electrochemically synthesized polypyrroles. *Synthetic Metals*, *117*(1–3), 45–51. https://doi.org/10.1016/S0379-6779(00)00537-3

Kumar, N., Kumar, V., Swart, H. C., Mishra, A. K., Catherine Ngila, J., & Parashar, V. (2015). Controlled microstructural hydrothermal synthesis of strontium selenides host matrices for EuII and EuIII luminescence. *Materials Letters*, *146*, 51–54. https://doi.org/10.1016/j.matlet.2015.01.150

Kundale, S. S., Kamble, G. U., Patil, P. P., Patil, S. L., Rokade, K. A., Khot, A. C., Nirmal, K. A., Kamat, R. K., Kim, K. H., An, H.-M., Dongale, T. D., & Kim, T. G. (2023). Review of Electrochemically Synthesized Resistive Switching Devices: Memory Storage, Neuromorphic Computing, and Sensing Applications. *Nanomaterials*, *13*(12), 1879. https://doi.org/10.3390/nano13121879

Lee, P. A., Said, G., Davis, R., & Lim, T. H. (1969). On the optical properties of some layer compounds. *Journal of Physics and Chemistry of Solids*, *30*(12), 2719–2729. https://doi.org/10.1016/0022-3697(69)90045-6

Mousavi, S. M., Raoof, J. B., & Ghani, M. (2023). Electrocatalysis of methanol at the surface of carbon paste electrode modified with composite of Cu-Al-layered double hydroxide and graphene oxide. *Journal of the Iranian Chemical Society*, *20*(9), 2285–2295. https://doi.org/10.1007/s13738-023-02836-4

Muhammad, Z., Ali, M. W., Mir, I. A., Khan, Q. U., & Zhu, L. (2020). Copper-doped induced ferromagnetic half-metal zirconium diselenide single crystals. *Nanotechnology*, *31*(23). https://doi.org/10.1088/1361-6528/ab72b3

Nag, J., Ryckman, J. D., Weiss, S. M., & Haglund, R. F. (2023). Silicon Photonics With Active (Phase Change) Materials for Optical Modulators. *Encyclopedia of Materials: Electronics*, *1–3*, V2-334-V2-352. https://doi.org/10.1016/B978-0-12-819728-8.00026-7

Peter Papoh, N. (2019). Introductory Chapter: Chalcogen Chemistry - The Footprint into New Materials Development. *Chalcogen Chemistry*. https://doi.org/10.5772/intechopen.82542